

Evaluation of Dry Protonated Calcium Alginate Beads for Biosorption Applications and Studies of Lead Uptake

Ricardo Lagoa · J. R. Rodrigues

Accepted: 3 May 2007 / Published online: 24 May 2007
© Humana Press Inc. 2007

Abstract Alginate polysaccharide is a promising biosorbent for metal uptake. Dry protonated calcium alginate beads for biosorption applications were prepared, briefly characterized and tested for lead uptake. Several advantages of this biosorbent are reported and discussed in comparison with other alginate-based sorbents. The alginate beads contained 4.7 mmol/g of COOH groups, which suffered hydrolysis near pH 4. The Weber and Morris model, applied to kinetic results of lead uptake, showed that intraparticle diffusion was the rate-controlling step in lead sorption by dry alginate beads. Equilibrium experiments were performed and the data were fitted with different isotherm models. The Langmuir equation was the most adequate to model lead sorption. The maximum uptake capacity (q_{\max}) was estimated as 339 mg/g and the Langmuir constant (b) as 0.84 l/mg. These values were compared with that of other sorbents found in the literature, indicating that dry protonated calcium alginate beads are among the best biosorbents for the treatment and recovery of heavy metals from aqueous streams.

Keywords Biosorption · Alginate · Lead · Heavy metal · Water treatment · Metal recovery · Polysaccharide

Introduction

The growing outspread of heavy metals in the environment and their serious toxicity to animals, plants, and microorganisms represent a major pollution concern. Several human activities, namely mining and metal processing industries, release to the environment wastewaters containing heavy metals such as lead, cadmium, and copper [1].

Industrial wastewaters with high concentrations of heavy metals are usually treated by chemical precipitation and coagulation techniques [1, 2]. However, these methods are

R. Lagoa (✉) · J. R. Rodrigues
School of Technology and Management, Polytechnic Institute of Leiria, Morro do Lena, Alto do Vieiro,
2411-901 Leiria, Portugal
e-mail: rlagoa@estg.iplleiria.pt

ineffective for low concentrations and produce hazardous wastes that need further treatment. Ion exchange and membrane technologies can reduce heavy metal concentrations to levels compatible with the increasing restrictions of environmental regulations, but their cost is a critical disadvantage [1–3].

Metal biosorption consists in the use of biological materials to uptake metals from solutions, and it has been suggested as an alternative method for the removal of heavy metals from wastewater. Many biosorbents of plant, animal, and microbial origin, including biopolymers such as chitin, agarose, and alginate, have been tested for metal sorption from aqueous solutions and industrial effluents [3–9].

Alginate is a major component of the cell wall of brown algae, and several authors have reported its affinity for heavy metals [9–14]. Alginate is a linear polysaccharide composed of β -D-mannuronic acid (M) and α -L-guluronic acid (G) residues. In an alginate chain, the M and G residues are distributed in repeating blocks of M residues (M blocks) and G residues (G blocks) interspersed by blocks of alternating M and G residues (MG blocks) [15]. Mannuronic and guluronic acid residues have carboxylic and hydroxyl functional groups that take part in metal binding to alginate [12–14]. In the presence of di- and trivalent cations, alginate solutions form a gel as a result of polymer interchain associations. According to the “egg-box” model for alginate gelation, cations such as calcium, barium, and copper ions cooperatively interact with G blocks forming ionic crosslinks between polymer chains. Sequences of polyguluronate pack together with the cations strongly coordinated in cavities between the chains causing gelation of the polysaccharide [16, 17].

Brown algae are an abundant source for alginate extraction and this biopolymer is commercially available. It is possible to obtain gel and dry alginate particles with different physical–chemical properties depending on the gelling conditions and subsequent treatments. These features, conjugated with a high capacity to bind heavy metals, make alginate a remarkable candidate for biosorption applications. Different sorts of alginate-based sorbents can be produced: dry or gel beads, with varying particle sizes, porosity, and mechanical strength, eventually entrapping biomass or other co-sorbent materials.

Alginate-based sorbents have been tested for the removal of several metal ions, such as Pb^{2+} , Hg^{2+} , Cd^{2+} , Cu^{2+} , Ni^{2+} , Co^{2+} , Mn^{2+} , and Cr^{3+} . In most studies, calcium alginate gel beads are used [5, 18–24]. These gel beads are produced by dispersing drops of an alginate solution in a calcium solution. Ibáñez and Umetsu [25] prepared calcium and barium alginate beads and, after having not found morphological differences between them, used the barium alginate beads for the uptake of several metals. These authors proposed protonation of the beads with an acid to generate carboxylic groups with labile protons suitable for exchange with metal ions. In addition, these authors suggested the use of dry beads instead of gel beads based on the assumptions of a better handling nature and that the channels formed during the drying process would enhance sorbent permeability and improve sorption. However, Chen et al. [20] compared the kinetics of copper ion uptake by dry and gel beads and found a greater uptake rate for gel beads.

Gotoh et al. [21] and Dhakal et al. [26] prepared sorbent particles for metal uptake using crosslinked alginate to improve the mechanical and chemical stability of alginate gel beads. Alginate particles for sorption were also prepared in combination with other materials: microbial biomass [5, 7, 19, 22, 27], chitosan [28], xanthan gum [24], and an ion-exchange resin [29]. Other metal-binding substances, such as humic acid [23], SDBS surfactant [30], and Cyanex 302 [31], were incorporated in alginate beads. A Ca alginate-based ion-exchange resin [32] and an alginate-coated cotton sorbent [24] were also tested as sorbents. Some authors removed heavy metals from wastewaters by direct addition of sodium alginate as an aqueous solution or as a powder [33, 34].

The aim of this work was to evaluate the suitability of dry protonated alginate particles for biosorption applications and to examine their potential for lead uptake from aqueous solutions. The preparation of dry protonated alginate beads was investigated and relevant characteristics of this sorbent were analyzed. The beads were tested for uptake of lead because this is an important toxic pollutant and there are few studies concerning lead uptake by alginate.

Materials and Methods

Chemicals

Sodium alginate used for sorbent preparation was purchased from Panreac. Calcium chloride ($\text{CaCl}_2 \cdot 2\text{H}_2\text{O}$) and sodium chloride (NaCl) were supplied by Merck. Nitric and hydrochloric acids were obtained from Riedel-de Haën and sodium hydroxide (NaOH) from Panreac. Lead nitrate [$\text{Pb}(\text{NO}_3)_2$] and lead standard solutions were obtained from Merck.

Preparation and Characterization of Alginate Beads

Sodium alginate 2% (w/w) aqueous solution was prepared by addition of a weighted amount of sodium alginate to a portion of water, followed by agitation in an orbital shaker for 3 h at 50°C. The alginate solution was added drop-by-drop, by using a peristaltic pump and a silicone tube with internal diameter 1.6 mm, to a 150-mM CaCl_2 stirred solution. The gel beads were kept in the CaCl_2 solution, with gentle agitation, for approximately 12 h for complete gelation.

The nonprotonated calcium alginate beads were obtained by removing the gel beads from the CaCl_2 solution and washing three times with deionized water. The protonated calcium alginate gel beads were prepared by transferring the nonprotonated ones to 1 M nitric acid for 24 h [25] and then by rinsing exhaustively with deionized water until washing water had a neutral pH. The dry beads were obtained by placing the gel beads in an oven at 35°C for 3 days. The dry beads were stored in a closed flask, at room temperature, and showed no visible signs of alteration after several months.

Dry weight percentage of the different types of alginate beads were measured after drying in an oven at 50°C for 24 h.

Dry beads were digitally imaged and the mean diameter of more than 200 beads was measured using the image analysis software ImageJ [35].

For the potentiometric titration, 0.200 g of dry protonated alginate beads was suspended in 100 ml of 1 mM NaCl . The mixture was titrated, under constant stirring, with a 0.1006-mM NaOH secondary standard solution. Measurements of pH were made with a Metrohm 692 pH meter equipped with a pH electrode and an Ag/AgCl reference electrode. After each addition of NaOH , the system was allowed to equilibrate and the pH was recorded when the rate of the linear drift was <0.01 pH/min.

The number of carboxylic (weak acid) groups per gram of sorbent, $[\text{COOH}]$ (mmol/g), was found using Eq. 1:

$$[\text{COOH}] = \frac{V_{\text{eq}} \cdot [\text{NaOH}]}{m}, \quad (1)$$

where V_{eq} (ml) is the equivalence volume, obtained from the maximum in the first derivative of the titration curve (which corresponds to the inflection point of the titration curve); $[\text{NaOH}]$ (mol/l) is the titrant concentration; and m (g) is the sorbent mass.

Sorption Equilibrium Studies

The assays to study equilibrium of lead sorption by alginate beads were carried out by adding weighted amounts of sorbent to flasks containing 25 ml of $\text{Pb}(\text{NO}_3)_2$ solution. The flasks were agitated in an orbital shaker at 300 rpm, 25°C , until equilibrium was attained. A solution sample was collected from each flask before the addition of the beads and after equilibrium was reached. The lead concentration was measured by atomic absorption spectroscopy, performed in a Varian SpectraAA spectrometer, with background correction.

The lead solution pH was adjusted to 5 with 0.1 M HCl or 0.1 M NaOH before addition of the beads. The pH was not controlled during the sorption assays. The amount of metal ions bound by alginate beads was determined according to Eq. 2:

$$q = \frac{(C_i - C_f) \cdot V}{m} \quad (2)$$

where q (mg/g) is the amount of lead ions bound per unit weight of alginate sorbent; C_i (mg/l) is the initial concentration of lead in the solution; C_f (mg/l) is the final lead concentration in the solution after sorption equilibrium was attained; V (l) is the solution volume; and m (g) is the sorbent mass. The quantity q was used throughout the work in the characterization of alginate beads, in the equilibrium isotherms, and in the kinetic studies.

Sorption Kinetic Studies

The kinetic assays were carried out in a stirred tank reactor (total volume = 1 dm^3) equipped with a two-blade impeller driven by a variable speed motor. The reactor was loaded with 500 ml of $\text{Pb}(\text{NO}_3)_2$ solution adjusted to pH 5 and the run was started with the addition of 100 mg of dry protonated alginate beads. At time intervals, solution samples were withdrawn for lead analysis.

Results and Discussion

Preparation and Characterization of Alginate Beads

Different sorts of alginate-based sorbents for metal ions uptake have been reported. However, a direct comparison between these sorbents and an evaluation based on their sorption potential and the physical–chemical characteristics relevant for practical application are often missing. In this work, three different types of alginate beads were prepared as potential biosorbents:

- Nonprotonated calcium alginate gel beads;
- Protonated calcium alginate gel beads;
- Dry protonated calcium alginate beads.

The nonprotonated calcium alginate gel beads were prepared using the conventional method of gel beads preparation for enzyme and cell entrapment, which is based on the

gelling properties of the polysaccharide. A sodium alginate solution is added, dropwise, to calcium ions that promote the reticulation of alginate chains, leading to the gelation of the drops in the form of calcium alginate beads.

When the gel beads are immersed in an acid solution, the carboxylic groups in M and G residues become protonated, releasing sodium and weakly bound calcium ions to the solution. The protonation caused a slight contraction of the gel beads (Table 1). This effect was observed in all batches of prepared beads and it can be explained by the decrease of the negative charges in the alginate chains. The protonation of the carboxylic groups reduces the electrostatic repulsion between polymer chains, allowing a closer approximation.

Table 1 shows that the gel beads contain predominantly water. The drying process removed most of the water from the beads and decreased considerably the particle size. The shrinkage observed after drying the gel beads is quite irreversible and the beads do not revert to gel state in aqueous medium. Dry beads swelled up approximately 5% when immersed for 7 days in water and in metal solutions (300 mg/l lead nitrate or 300 mg/l copper sulphate).

The particle size of the sorbents is an important variable and a full-scale application requires granulated sorbents with an adequate sizing [1]. The method for alginate beads preparation offers two ways to adjust the final particle size: in the gelation step, the size of the drops of alginate solution or the calcium concentration can be changed (which also alters permeability and rigidity [36]); after the drying step, the particles can be ground and sieved to obtain the desired size. Figure 1 shows a picture and the size distribution of the dry protonated alginate beads prepared in this work. The particle sizes are distributed over a rather narrow range. The mean diameter of dry beads is 1.16 ± 0.05 mm, which is in the range recommended for sorbents to be used in fixed-bed columns [1].

Dry alginate beads are very convenient to store and transport when necessary. They are also more resistant to biological deterioration and have a higher number of binding sites per unit volume and mass than their wet gel counterparts. Furthermore, the gel beads are too fragile, which make their handling in large quantities difficult, and they lack the necessary rigidity to support the pressure in a large-scale sorption column.

Some authors introduce a protonation step in alginate beads preparation [21, 25, 28, 37], assuming that protonated beads have greater metal uptake capacity than the nonprotonated ones. However, this difference was only reported for chromium sorption [25]. To clarify this question, sorption assays were carried out with dry beads in two forms: protonated and nonprotonated (Fig. 2).

The comparison between the uptake capacities of the two types of alginate beads shows that the protonated beads have a larger binding capacity, although the results are very similar for low metal concentrations. The use of protonated beads has an additional advantage related to the regeneration of the sorbent. After uptake of metal ions from solutions, metals should be desorbed for possible recovery and the saturated biosorbent regenerated for reuse. Desorption has been attempted with different desorbing agents and the best results were obtained with HCl and HNO₃ [18, 22, 24]. The acid solution

Table 1 Dry weight and mean diameter of calcium alginate beads.

Type of beads	Dry weight (%)	Mean diameter (mm)
Nonprotonated gel beads	3.7	3.1
Protonated gel beads	3.4	3.0
Dry protonated beads	89.6	1.16

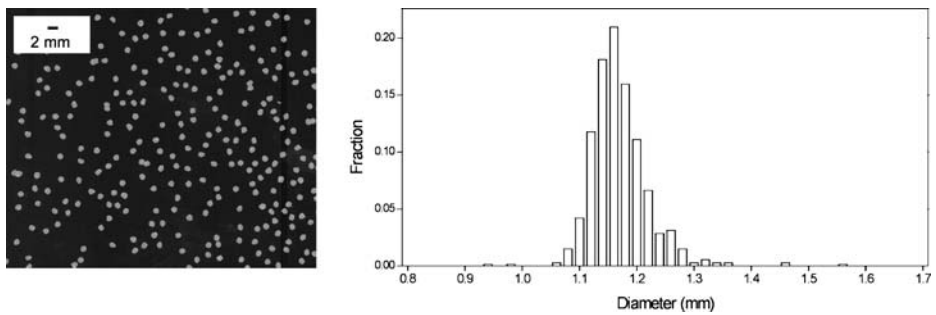


Fig. 1 Picture and size distribution of dry protonated calcium alginate beads

regenerates the alginate sorbent in the protonated form for the next uptake cycles. Therefore, it is worthwhile to characterize the sorption behavior of the protonated beads for industrial large-scale metal recovery.

Metal uptake by alginate is mainly due to the carboxylic groups of mannuronic and guluronic acid residues in the polysaccharide chains. The sorbent capacity depends on the number and acid-base profile of the binding sites. Figure 3 shows the potentiometric titration curve of the dry protonated alginate beads. The wide plateau in the pH range 4–5 reveals the abundance of acid groups in the sorbent. With the gradual addition of NaOH throughout the titration, acid groups become progressively deprotonated, according to their dissociation constants (K_a), buffering the addition of base. The plateau corresponds to an apparent pK_a value of 4.2, which is about 0.7 pH units higher than the value reported for alginic acid [13]. This suggests that carboxylic groups in dry calcium alginate beads behave as weaker acids than in alginic acid. A slight decrease of 0.15 pH units is observed after addition of 0.20 mmol NaOH. The carboxylic groups in contact with the solvent are probably the first ones to be deprotonated upon the addition of base. The build-up of negative charges leads to increasing electrostatic repulsion between deprotonated carboxylic groups that results in the loss of integrity of alginate beads. This event subsequently induces exposure of buried carboxylic groups to the solvent, decreasing their apparent pK_a . The dissociation of these stronger acid groups decreases the solution pH. This view is consistent with the progressive disruption of the beads observed for higher volumes of NaOH added. At basic pH, the beads were completely dissolved as a turbid solution.

Fig. 2 Lead uptake capacity of protonated and nonprotonated dry calcium alginate beads for different initial metal concentrations. Alginate beads (40 mg) were added to 25 ml of lead solution and sorption evolved under orbital shaking, 300 rpm, 25°C, for 3 h

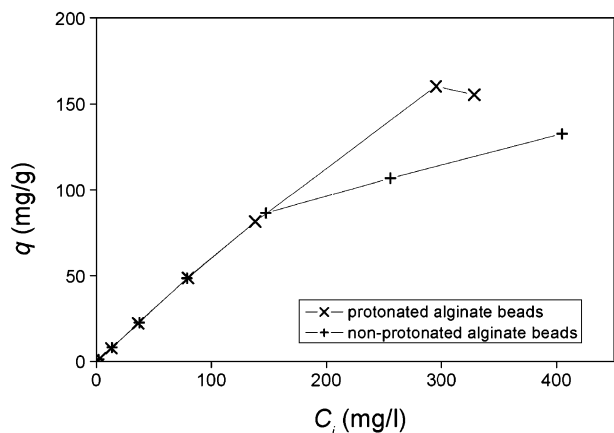
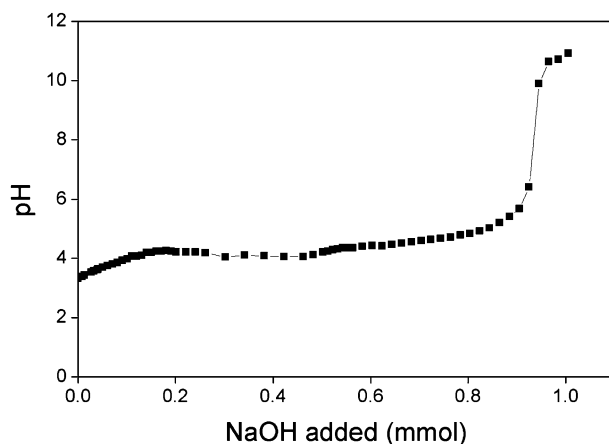


Fig. 3 Potentiometric titration curve of dry protonated calcium alginate beads



The number of carboxylic acid groups in the alginate beads is 4.7 mmol/g, which is superior to two other reported alginate preparations: 4.4 mmol/g [13] and 3.338 mmol/g [32]. However, the carboxylic acid content obtained is inferior to the estimate (5.1 mmol/g) calculated from the alginate monomer content and the dry weight of the beads (Table 1), probably because of impurities in the alginate sample.

Sorption Kinetics

In processes of heavy metal removal, the initial uptake rate is a very important factor for reactor design and process optimization [38]. Figure 4 shows the evolution of lead uptake by dry protonated alginate beads from solutions with different metal concentrations and under different stirring rates. The process of metal ions adsorption by an adsorbent can be divided into four steps [4, 39]: (1) transport of metal ions from the bulk solution to the exterior film surrounding the sorbent; (2) movement of metal ions across the external liquid film boundary layer to the adsorbent external surface; (3) migration of metal ions through the pores of the sorbent by intraparticle diffusion; and (4) adsorption at internal binding sites. In a fully mixed agitated tank, step 1 is fast and is usually ignored. Adsorption to surface sites (step 4) is also considered a rapid event. Thus, these steps usually are not considered rate-limiting in the sorption processes [4]. Transport to the adsorbent particle (steps 1 and 2) depends on the agitation of the mixture. The results show that the agitation rate does not significantly influence sorption kinetics, suggesting that the rate-controlling step is diffusion in the adsorbent interior (internal mass transfer).

A common approach to identify the mechanism involved in the adsorption process is by fitting an intraparticle diffusion plot [39, 40]. According to the model proposed by Weber and Morris for intraparticle diffusion [41], sorption can be modeled by Eq. 3:

$$q = K \cdot \sqrt{t}, \quad (3)$$

where q is the amount of adsorbate bound per unit weight of adsorbent at time t and K is the intraparticle diffusion rate constant. When intraparticle diffusion is the rate-limiting step, q varies linearly with $t^{1/2}$ and K can be estimated from the slope of the line [41]. Several authors [4, 39, 40, 42] have reported plots with multilinearity, or with curved and linear portions, representing the sequential stages of mass transfer of the solute onto the adsorbent.

Fig. 4 Time course of lead uptake by dry protonated calcium alginate beads from solutions with various initial lead concentrations under different stirring speeds. Alginate beads (100 mg) were added to 500 ml lead solution and sorption proceeded with mechanical agitation. Initial lead concentrations and stirring speeds are indicated in the plots

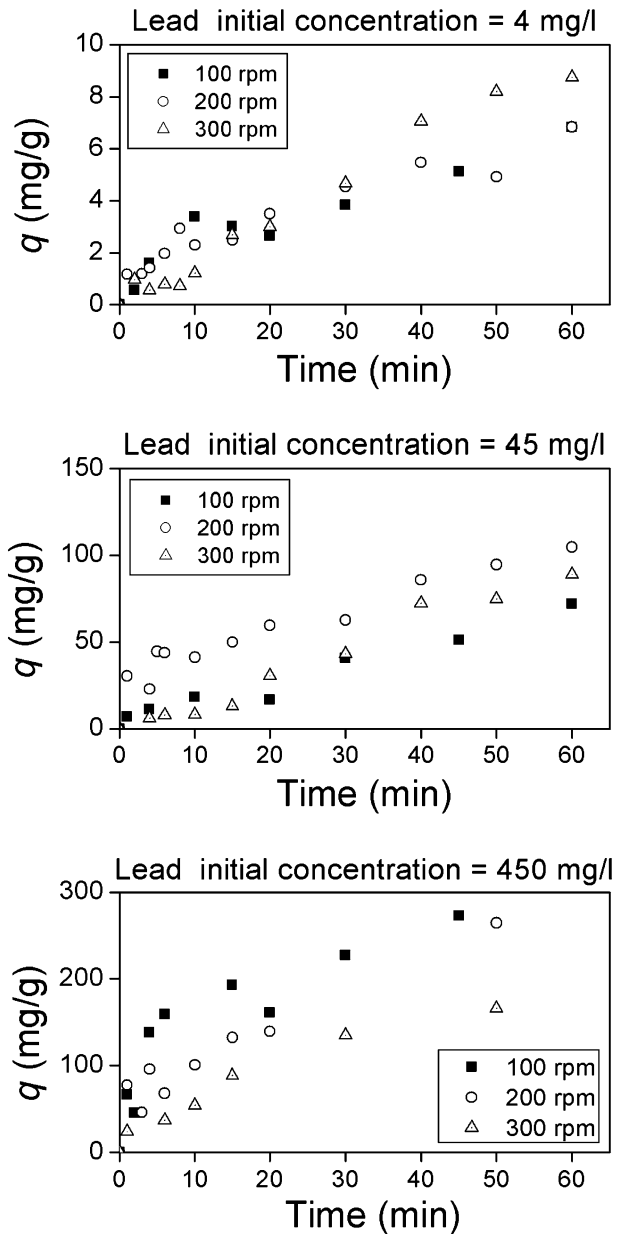
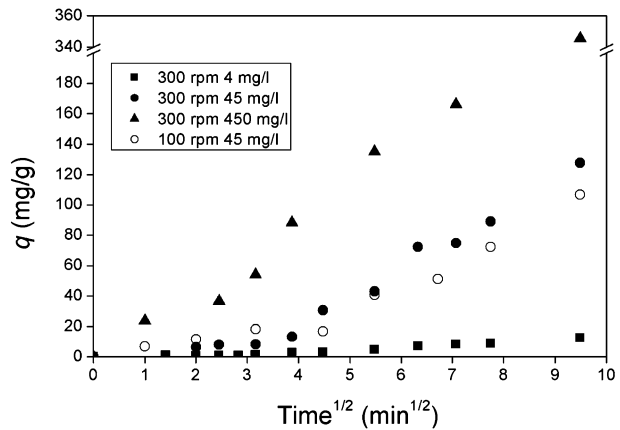


Figure 5 illustrates some examples of intraparticle diffusion plots of the kinetic data obtained in this work. The plots show two regions. The initial portion is linear or slightly curved and corresponds to the early moments of sorption. During this stage, internal mass transfer is negligible and film diffusion from the bulk solution to the sorbent surface is the main process. The later region of the plots is approximately linear, suggesting that intraparticle diffusion becomes the rate-controlling process.

Fig. 5 Intraparticle diffusion plots for the sorption of lead by dry protonated calcium alginate beads at different initial lead concentrations and stirring speeds



The intraparticle diffusion rate constants (K), computed from the slope of the later portion of the plots, are presented in Table 2. These rate constants depend strongly on the initial Pb^{2+} concentration. Intraparticle diffusion is faster for higher metal concentration because of the larger concentration gradient between the particle superficial film and the internal pore solution.

The agitation rate had little effect in the diffusion rate constants, confirming that diffusion within the pores of the sorbent particles offers the major resistance to lead transfer and sorption.

Chen et al. [20] found that external mass transport affects the initial phase in copper sorption by gel and dry alginate beads, whereas diffusion influences the later phase. A diffusion-controlled model provided a good representation of sorption kinetics, assuming a higher diffusivity in gel beads than in dry beads. According to the authors, gel beads have a faster uptake rate because mass transport is determined by diffusion in water and gel beads contain mostly water. The kinetic results obtained by Park and Chae [24] with different alginate sorbents also suggest the importance of intraparticle diffusion. Lead sorption by cotton coated with an alginate gel film was much faster than sorption by alginate beads or capsules, and the time to reach equilibrium could be reduced with thinner gel films.

Sorption Equilibrium

Equilibrium assays were done to characterize the sorption capacity of the dry protonated alginate beads. The results were fitted with the equations from four adsorption isotherm models. The specific physical–chemical assumptions of these models are probably not

Table 2 Intraparticle diffusion rate constants (K , (mg/g) min^{-1/2}), according to the Weber and Morris model, for lead sorption by dry protonated calcium alginate beads with different initial lead concentrations and stirring speeds.

Stirring speed (rpm)	C_i (mg/l)		
	4	45	450
100	0.9	17	38
200	1.0	14	38
300	1.8	19	41

fulfilled by the present sorption system. Therefore, the applicability of the adsorption isotherms should be considered only as a mathematical representation of the sorption equilibrium, and no mechanistic conclusions can be addressed from the fit of the equations alone. In spite of these limitations, the models allow the calculation of metal uptake capacities, which are useful for comparisons between different metals and sorbents. The following isotherm models were used to fit the results: the Langmuir model [43],

$$q_e = \frac{q_{\max} \cdot b \cdot C_e}{1 + b \cdot C_e} \quad (4)$$

the Freundlich model [44],

$$q_e = K_F \cdot C_e^{1/n} \quad (5)$$

the Redlich–Peterson model [45],

$$q_e = \frac{K_{RP} \cdot C_e}{1 + a_{RP} \cdot C_e^\beta} \quad (6)$$

and the Koble–Corrigan model [46],

$$q_e = \frac{A \cdot C_e^n}{1 + B \cdot C_e^n}, \quad (7)$$

where q_e (mg/g) is the amount of metal bound per unit weight of sorbent at equilibrium; C_e (mg/l) is the lead ions concentration at equilibrium; q_{\max} (mg/g) is the maximum metal uptake capacity; b (l/mg) is the Langmuir constant; K_F [(mg/g) (mg/l)^{-1/n}] and n (–) in Eq. 5 are the Freundlich constants; K_{RP} (l/g) and a_{RP} [(l/mg)^β] are the Redlich–Peterson constants; β (–) is the Redlich–Peterson exponent; A [(mg/g) (mg/l)⁻ⁿ] and B [(l/mg)ⁿ] are the Koble–Corrigan constants; and n (–) in Eq. 7 is the Koble–Corrigan exponent.

The experimental results are shown in Fig. 6 and the parameters from fitting Eq. 4 to 7 are in Table 3. The Freundlich model has the lowest coefficient of determination (R^2), which makes it the least suitable to describe lead sorption by dry protonated alginate beads. Three-parameter models, such as the Redlich–Peterson and Koble–Corrigan models, are expected to fit the data better, and indeed they have higher R^2 values in comparison to the Freundlich model, although similar to the two-parameter Langmuir model. However, the

Fig. 6 Biosorption isotherm of lead onto dry protonated calcium alginate beads. Alginate beads (5 or 10 mg) were added to 25 ml of lead solution with different concentrations. Sorption evolved under orbital shaking, 300 rpm, 25 °C, for 24 h. The bars represent the standard error of the mean of triplicate assays. The curve was obtained by fitting the data points to the Langmuir model (Eq. 4)

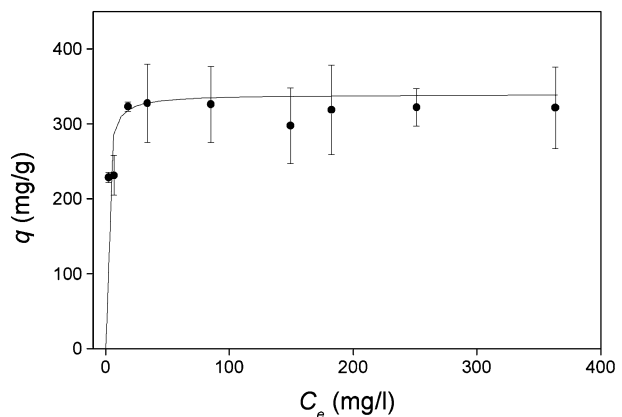


Table 3 Estimated parameters from the Langmuir, Freundlich, Redlich–Peterson, and Koble–Corrigan models for lead sorption by dry protonated calcium alginate beads.

Model	Parameters		R^2	MRE (%)
Langmuir	$q_{\max}=339$ mg/g	$b=0.84$ l/mg	0.945	13
Freundlich	$K_F=224$ (mg/g) (mg/l) $^{-1/n}$	$n=9.94$	0.689	12
Redlich–Peterson	$K_{RP}=285$ l/g	$a_{RP}=0.84$ (l/mg) $^\beta$	$\beta=1.000$	29
Koble–Corrigan	$A=269$ (mg/g) (mg/l) $^{-n}$	$B=0.80$ (l/mg) n	$n=1.085$	48

R^2 —coefficient of determination

MRE—maximum relative standard error

maximum relative standard error (MRE) of the parameters obtained for the Redlich–Peterson and the Koble–Corrigan models are high. This indicates that although the models fit the data well, the parameters are ill-defined. Moreover, the parameter β of the Redlich–Peterson model obtained from the fit is equal to 1.000, which causes the corresponding equation to simplify to the Langmuir one. Therefore, based on the R^2 and MRE values, the Langmuir model is the most appropriate to describe sorption of lead by dry protonated alginate beads.

Although the Langmuir model is the most adequate of the tested models, Fig. 6 shows slight deviations of some data points from the model prediction. This may be caused by the variation of solution pH during sorption that alters the effect of proton competition for the binding sites in alginate. The initial pH was 5 in all experiments, but pH varies during sorption because metal uptake is accompanied by proton release to solution.

The maximum binding capacity of the sorbent, obtained from the Langmuir model, is 339 mg/g (1.64 mmol/g), which is in agreement with the experimental results (Table 3 and Fig. 6). A maximum binding capacity of 2.35 mmol/g can be expected based on COOH content of the beads obtained from the titration curve (4.7 mmol/g) and assuming that each lead ion occupies two COOH groups. The measured value was lower, possibly because not all COOH groups from mannuronic and guluronic residues in alginate are active sites for metal uptake, as suggested by some authors [13, 36, 47].

Comparison with other Sorbents

Table 4 summarizes the parameters for lead uptake with alginate-based sorbents and with some of the best lead sorbents described in the literature. The Langmuir parameters q_{\max} and b are used for comparison when available, as well as q_{10} , which is a useful indicator of the uptake capacity with low metal concentration [38].

The calcium alginate-based ion-exchange resin (CABIER) produced by Chen et al. [32] is the alginate-based sorbent with the highest reported sorption capacity for lead (Table 4). Bayramoğlu et al. [19] studied lead uptake by alginate gel beads and by microalgae *Chlamydomonas reinhardtii* immobilized in alginate gel beads. The entrapment of the microalgae increased q_{\max} from 286 to 384 mg Pb $^{2+}$ /g biosorbent, but the sorption capacities at low metal concentration are similar. Alginate gel beads with entrapped *Pleurotus ostreatus* [27] also have a small uptake capacity in the presence of low lead concentrations (Table 4).

Dhakar et al. [26] investigated the adsorption behavior of crosslinked pectic and alginic acids, and their amide derivatives, in comparison to the cation exchange resin DIAION

Table 4 Lead uptake capacities of alginate-based sorbents and of some other sorbents selected from the literature.

Sorbent	q_{\max} (mg/g)	b^a (l/mg)	q_{10}^b (mg/g)	Reference
Alginate-based sorbents				
Alginate dry beads	339	0.84	303	This work
Alginate gel beads	286	–	–	[19]
Ca alginate-based ion-exchange resin	622	–	~600 ^c	[32]
Crosslinked alginic acid	249	–	–	[26]
<i>Pleurotus ostreatus</i> in alginate gel beads	121	4.6×10^{-3}	5.3	[27]
Other sorbents				
Cellulose/chitin beads	176	1.88×10^{-3}	3.2	[48]
Pestan	~120 ^c	–	~25 ^c	[49]
<i>Aureobasidium pullulans</i>	~200 ^c	–	170.4	[38]
<i>Mucor rouxii</i>	769	0.038	212	[50]
<i>Pseudomonas pseudoalcaligenes</i>	272	0.46	223	[51]
<i>Ascophyllum nodosum</i>	287	–	–	[52]
<i>Sargassum fluitans</i>	369	–	–	[52]
<i>Sargassum sp.</i>	258	0.147	154	[53]
Ion-exchange resin SK1B	–	–	167.7	[38]
Ion-exchange resin DIAION WK10	203	–	–	[26]

^a Parameter b from the Langmuir model (Eq. 4)

^b q_{10} is the lead uptake for 10 mg/l Pb^{2+} equilibrium concentration.

^c Estimated from the graphical representation of the results

WK10. Crosslinked alginic acid had a maximum sorption capacity of 249 mg/g, which was higher than alginic acid amide and the ion-exchange resin. Other polysaccharide materials such as cellulose/chitin beads [48] and Pestan, a fungal extracellular polysaccharide [49], have lower affinity for lead ions than alginate beads (Table 4).

Suh and Kim [38] compared the removal of lead from aqueous solutions with several sorbents, namely, an ion-exchange resin (SK1B), a zeolite, activated carbon, activated sludge, and biomass from *Aureobasidium pullulans* and *Saccharomyces cerevisiae*. The resin and *A. pullulans* biomass yielded the best q_{10} values (Table 4). A comparative investigation on lead biosorption by fungal biomass revealed the very high maximum uptake capacity of *Mucor rouxii*, 769 mg/g [50]. Leung et al. [51] isolated 12 bacterial species from activated sludge and obtained their sorption capacity for copper, nickel, and lead. The best results were achieved with *Pseudomonas pseudoalcaligenes*, which showed a maximum biosorption capacity of 271.7 mg Pb^{2+} /g dry cell.

Many algae are able to bind large amounts of metal ions [8, 9]. Leusch et al. [52] found q_{\max} values for lead uptake of 369 mg/g and 287 mg/g with *Sargassum fluitans* and *Ascophyllum nodosum*, respectively. In another study with *Sargassum sp.*, a maximum sorption capacity of 258 mg/g is reported [53] (Table 4).

The metal uptake capacities of several biosorbents have been reviewed by different authors [3, 6, 8, 9]. Alginate-based sorbents show higher binding capacities than most of the ion-exchange resins and algal, fungal, and bacterial biosorbents. Alginate dry protonated particles prepared in this work have a larger sorption capacity than the traditional gel beads and are comparable to the best lead sorbents reported.

Conclusions

The method for alginate beads preparation allows the production of different types of alginate sorbents. Nonprotonated and protonated alginate beads, in gel and dry states, were prepared and evaluated, having in mind their practical use in biosorption systems. The sorption potential and the physical–chemical properties of dry protonated alginate beads render them the most suitable for sorption applications.

Metal uptake by a porous particulate sorbent requires mass transfer from the bulk solution to the sorbent particle, intraparticle diffusion, and adsorption to a binding site. Kinetic data from lead sorption by dry alginate beads show that the process is greatly limited by intraparticle diffusion. For an optimized performance of the sorbent, internal mass transfer must be improved. The gelation conditions can be manipulated to produce smaller and more porous beads, which facilitate metal diffusion.

The sorption equilibrium was modeled with the Langmuir, Freundlich, Redlich–Peterson, and Koble–Corrigan equations. Sorption of lead by dry protonated calcium alginate beads is best described by the Langmuir equation. The maximum uptake capacity (q_{\max}), estimated as 339 mg lead/g sorbent, is comparable to the highest values found in the literature. As such, dry alginate beads are a promising biosorbent for lead removal from contaminated waters.

References

1. Volesky, B. (2001). *Hydrometallurgy*, 59, 203–216.
2. Kumiawan, T. A., Chan, G. Y. S., Lo, W. H., & Babel, S. (2006). *Chemical Engineering Journal*, 118, 83–98.
3. Ahluwalia, S. S., & Goyal, D. (2007). *Bioresource Technology*, 98, 2243–2257.
4. Choy, K. K. H., Ko, D. C. K., Cheung, C. W., Porter, J. F., & McKay, G. (2004). *Journal of Colloid and Interface Science*, 271, 284–295.
5. Aksu, Z., Eğretli, G., & Kutsal, T. (1998). *Process Biochemistry*, 33, 393–400.
6. Bailey, S. E., Olin, T. J., Bricka, R. M., & Adrian, D. D. (1999). *Water Research*, 33, 2469–2479.
7. Gupta, R., Ahuja, P., Khan, S., Saxena, R. K., & Mohapatra, H. (2000). *Current Science*, 78, 967–973.
8. Mehta, S. K., & Gaur, J. P. (2005). *Critical Reviews in Biotechnology*, 25, 113–152.
9. Davis, T. A., Volesky, B., & Mucci, A. (2003). *Water Research*, 37, 4311–4330.
10. Davis, T. A., Llanes, F., Volesky, B., Diaz-Pulido, G., McCook, L., & Mucci, A. (2003). *Applied Biochemistry and Biotechnology*, 10, 75–90.
11. Haug, A. (1961). *Acta Chemica Scandinavica*, 15, 1794–1795.
12. Emmerichs, N., Wingender, J., Flemming, H. C., & Mayer, C. (2004). *International Journal of Biological Macromolecules*, 34, 73–79.
13. Lamelas, C., Avaltroni, F., Benedetti, M., Wilkinson, K. J., & Slaveykova, V. I. (2005). *Biomacromolecules*, 6, 2756–2764.
14. Rodrigues, J. R., & Lagoa, R. (2006). *Journal of Carbohydrate Chemistry*, 25, 219–232.
15. Haug, A., Larsen, B., & Smidsrod, O. (1974). *Carbohydrate Research*, 32, 217–225.
16. Grant, G. T., Morris, E. R., Rees, D. A., Smith, P. J. C., & Thom, D. (1973). *FEBS Letters*, 32, 195–198.
17. Morris, E. R., Rees, D. A., Thom, D., & Boyd, J. (1978). *Carbohydrate Research*, 66, 145–154.
18. Abu Al-Rub, F. A., El Naas, M. H., Benyahia, F., & Ashour, I. (2004). *Process Biochemistry*, 39, 1767–1773.
19. Bayramoğlu, G., Tuzun, I., Celik, G., Yilmaz, M., & Arica, M. Y. (2006). *International Journal of Mineral Processing*, 81, 35–43.
20. Chen, J. P., Tendeyong, F., & Yiacoumi, S. (1997). *Environmental Science & Technology*, 31, 1433–1439.
21. Gotoh, T., Matsushima, K., & Kikuchi, K. I. (2004a). *Chemosphere*, 55, 57–64.
22. Kaçar, Y., Arpa, C., Tan, S., Denizli, A., Genç, Ö., & Arica, M. Y. (2002). *Process Biochemistry*, 37, 601–610.
23. Pandey, A. K., Pandey, S. D., & Misra, V. (2002). *Ecotoxicology and Environmental Safety*, 52, 92–96.
24. Park, H. G., & Chae, M. Y. (2004). *Journal of Chemical Technology and Biotechnology*, 79, 1080–1083.
25. Ibáñez, J. P., & Umetsu, Y. (2002). *Hydrometallurgy*, 64, 89–99.

26. Dhakal, R. P., Ghimire, K. N., Inoue, K., Yano, M., & Makino, K. (2005). *Separation and Purification Technology*, 42, 219–225.
27. Xiangliang, P., Jianlong, W., & Daoyong, Z. (2005). *Process Biochemistry*, 40, 2799–2803.
28. Gotoh, T., Matsushima, K., & Kikuchi, K. I. (2004b). *Chemosphere*, 55, 135–140.
29. Jodra, Y., & Mijangos, F. (2003). *Environmental Science & Technology*, 37, 4362–4367.
30. Karagunduz, A., Kaya, Y., Keskinler, B., & Once, S. (2006). *Journal of Hazardous Materials*, 131, 79–83.
31. Ocio, A., Mijangos, F., & Elizalde, M. (2006). *Journal of Chemical Technology & Biotechnology*, 81, 1409–1418.
32. Chen, J. P., Hong, L. A., Wu, S. N., & Wang, L. (2002). *Langmuir*, 18, 9413–9421.
33. Jang, L. K., Lopez, S. L., Eastman, S. L., & Pryfogle, P. (1991). *Biotechnology and Bioengineering*, 37, 266–273.
34. Fatin-Rouge, N., Dupont, A., Vidonne, A., Dejeu, J., Fievet, P., & Foissy, A. (2006). *Water Research*, 40, 1303–1309.
35. Rasband, W. S. (1997–2006) Image J, U. S. National Institutes of Health, Bethesda, Maryland, USA, <http://rsb.info.nih.gov/ij/>.
36. Mørch, Ý. A., Donati, I., Strand, B. L., & Skjåk-Bræk, G. (2006). *Biomacromolecules*, 7, 1471–1480.
37. Ibáñez, J. P., & Umetsu, Y. (2004) *Hydrometallurgy*, 72, 327–334.
38. Suh, J. H., & Kim, D. S. (2000). *Journal of Chemical Technology and Biotechnology*, 75, 279–284.
39. Ho, Y. S., Ng, J. C. Y., & McKay, G. (2000). *Separation and Purification Methods*, 29, 189–232.
40. Kalavathy, M. H., Karthikeyan, T., Rajgopal, S., & Miranda, L. R. (2005). *Journal of Colloid and Interface Science*, 292, 354–362.
41. Weber, W. J., & Morris, J. C. (1963). *Journal of the Sanitary Engineering Division, American Society of Civil Engineers*, 89, 31–39.
42. Sun, Q. Y., & Yang, L. Z. (2003). *Water Research*, 37, 1535–1544.
43. Langmuir, I. (1918). *Journal of the American Chemical Society*, 40, 1361–1403.
44. Freundlich, H. (1907). *Zeitschrift für Physikalische Chemie*, 57, 385–470.
45. Redlich, O., & Peterson, D. L. (1959). *Journal of Physical Chemistry*, 63, 1024.
46. Koble, R. A., & Corrigan, T. E. (1952). *Industrial and Engineering Chemistry*, 44, 383–387.
47. Davis, T. A., Llanes, F., Volesky, B., & Mucci, A. (2003). *Environmental Science & Technology*, 37, 261–267.
48. Zhou, D., Zhang, L. N., Zhou, J. P., & Guo, S. L. (2004). *Water Research*, 38, 2643–2650.
49. Moon, S. H., Park, C. S., Kim, Y. J., & Park, Y. I. (2006). *Process Biochemistry*, 41, 312–316.
50. Lo, W., Chua, H., Lam, K. H., & Bi, S. P. (1999). *Chemosphere*, 39, 2723–2736.
51. Leung, W. C., Chua, H., & Lo, W. H. (2001). *Applied Biochemistry and Biotechnology*, 91-3, 171–184.
52. Leusch, A., Holan, Z. R., & Volesky, B. (1996). *Applied Biochemistry and Biotechnology*, 61, 231–249.
53. Martins, B. L., Cruz, C. C. V., Luna, A. S., & Henriques, C. A. (2006). *Biochemical Engineering Journal*, 27, 310–314.